Transcranial Direct Current Stimulation-Based Neuromodulation Improves the Performance of Brain–Computer Interfaces Based on Steady-State Visual Evoked Potential

Shangen Zhang, Xiaorong Gao, *Member, IEEE*, Hongyan Cui, and Xiaogang Chen, *Member, IEEE*

***Abstract*— The study of brain state estimation and intervention methods is of great significance for the utility of brain-computer interfaces (BCIs). In this paper, a neuromodulation technology using transcranial direct current stimulation (tDCS) is explored to improve the performance of steady-state visual evoked potential (SSVEP)-based BCIs. The effects of pre-stimulation, sham-tDCS and anodal-tDCS are analyzed through a comparison of the EEG oscillations and fractal component characteristics. In addition, in this study, a novel brain state estimation method is introduced to assess neuromodulation-induced changes in brain arousal for SSVEP-BCIs. The results suggest that tDCS, and anodal-tDCS in particular, can be used to increase SSVEP amplitude and further improve the performance of SSVEP-BCIs. Furthermore, evidence from fractal features further validates that tDCS-based neuromodulation induces an increased level of brain state arousal. The findings of this study provide insights into the improvement of BCI performance based on personal state interventions and provide an objective method for quantitative brain state monitoring that may be used for EEG modeling of SSVEP-BCIs.**

***Index Terms*— Steady-state visual evoked potential (SSVEP), brain–computer interface (BCI), transcranial direct current stimulation (tDCS), neuromodulation, brain state.**

Manuscript received 21 October 2022; revised 3 January 2023 and 7 February 2023; accepted 11 February 2023. Date of publication 14 February 2023; date of current version 24 February 2023. This work was supported in part by the National Key Research and Development Program of China under Grant 2022YFC3602803, in part by the National Natural Science Foundation of China under Grant U2241208 and Grant 62171473, in part by the Fundamental Research Funds for the Central Universities of China under Grant FRF-TP-20-017A1, and in part by the Tianjin Municipal Science and Technology Plan Project 21JCYBJC01500. *(Corresponding author: Xiaogang Chen.)*

This work involved human subjects or animals in its research. Approval of all ethical and experimental procedures and protocols was granted by the Institutional Review Board of Tsinghua University under Approval No. 20180041.

Shangen Zhang is with the School of Computer and Communication Engineering, University of Science and Technology Beijing, Beijing 100083, China (e-mail: zhangsfphd@163.com).

Xiaorong Gao is with the Department of Biomedical Engineering, Tsinghua University, Beijing 100084, China (e-mail: gxr-dea@tsinghua.edu.cn).

Hongyan Cui and Xiaogang Chen are with the Institute of Biomedical Engineering, Chinese Academy of Medical Sciences and Peking Union Medical College, Tianjin 300192, China (e-mail: cuihy@bme.cams.cn; chenxg@bme.cams.cn).

Digital Object Identifier 10.1109/TNSRE.2023.3245079

I. Introduction

SIGNIFICANT progresses have been made in steady-state visual evoked potentials (SSVEP)-based brain-computer interfaces (BCIs) with improvements in stimulus encoding methods and neural decoding algorithms [1], [2], [3]. However, high-intensity visual stimulation and high-load cognitive activity may cause changes in human states and consequently a decline in BCI system performance. Decreased levels of brain arousal, such as when fatigue sets in, may lead not only to slower responses and reduced attention, but also to decreased signal quality and reduced system classification performance [4], [5]. To address the challenges of reduced system robustness and reduced effective work time due to reduced levels of brain arousal, the study of brain state estimation and intervention methods is of great significance for the utility of BCI systems.

Transcranial direct current stimulation (tDCS)-based neuromodulation is an effective method of brain state intervention, and has the potential to enhance the classification accuracy of BCIs. tDCS is a non-invasive technique that uses a low-intensity, constant, direct current (1-2 mA). tDCS modulates cortical excitability through the mechanism of hyperpolarization or depolarization of the resting membrane potential, which depends on the polarity of the stimulus [6], [7]. tDCS is commonly used in the studies of rehabilitation and functional brain disorders. However, research in the area of BCI remains in its infancy.

Researchers have found that tDCS can modulate irritability and sustain oscillatory activity in the cerebral cortex, which allows the improvement of neural response during BCI tasks. For example, tDCS has been used to increase P300 response, decrease P300 latency, and generally enhance the accuracy of target detection in P300-BCI systems [8]. Anodal-tDCS has led to improved P300-BCI spelling performance in neurologically impaired subjects [9]. In sensorimotor rhythm-based BCIs, the orientation interactivity was changed through tDCS interaction during non-exogenous activities [10].

However, the results seem to be unsatisfactory when it comes to the enhancement of the target detection accuracy of SSVEP-BCIs based on tDCS. For example, anodal-tDCS significantly enhanced EEG features for electrodes with low signal-to-noise ratio (SNR) values before tDCS, but the enhancement was not obvious in locations with higher SNRs [11]. Compared to the sham-tDCS mode, anodal-tDCS increased the SSVEP energy at 10 Hz, while both anodal-tDCS and cathode-tDCS significantly decreased the SSVEP energy at 7 Hz [12]. In addition to this, while most studies reported enhanced and reduced cortical excitability through anodal- and cathodal-tDCS, respectively [13], [14], some studies also reported opposite results [15], [16]. The shortcomings of previous studies and the potential of neuromodulation techniques have made the investigation of techniques to enhance the target detection accuracy of SSVEP-BCI using tDCS both urgent and relevant.

Considering the inadequacies of past studies, in this paper, the authors attempt to explore tDCS-based neuromodulation technology to improve the target detection accuracy of SSVEP-BCIs efficiently. The EEG characteristics under pre-stimulation, sham-tDCS and anodal-tDCS are compared to verify the neuromodulation effect. The experiments are divided into offline and online experiments, where the former experiments investigate the effect of tDCS on SSVEP characteristics and are used to determine the optimal tDCS stimulation scheme, while the latter experiments introduce real-time feedback to verify the impact of tDCS on BCI performance. The EEG characteristics under different modes are compared, including not only oscillatory features such as envelopes, amplitude and classification accuracy of SSVEP, but also fractal features reflecting the characteristics of brain states, thus validating the effectiveness of the neuromodulation methods more comprehensively.

To address the shortcomings of traditional brain state assessment methods, a new brain state assessment method not yet used in SSVEP-BCI is introduced to verify the neuromodulation's efficacy on brain state intervention. Narrow-band energy spectrum distribution is the most widely used method for brain state assessment. It has been shown that EEG energy from 0.5 Hz to 8 Hz is enhanced as human enters a fatigue state [17], [18]. The levels of brain arousal were assessed through the energy integration indicators of alpha, beta, theta and their entropies [19]. Other researchers assessed brain states through the integration of multiple entropies of the raw electroencephalogram [20]. However, in the application scenario of SSVEP-BCIs, the energy of the oscillatory component changed drastically and the conclusions of the narrow-band energy spectrum distribution were distorted and not robust. In the case of SSVEP-BCIs, the frequency energy associated with target flicker was obviously disturbed when subjects received visual stimuli, which led to biased brain state estimates when raw EEG data were used. In addition, another drawback of narrow-band spectral energy is its non-intuitive and unreliable nature, which is due to the difficulty of describing the variation of energy with frequency in a holistic manner and providing quantitative and robust measurements of brain states. To address these shortcomings of traditional brain state assessment methods, in this study the Irregular Sampling Automatic Spectral Analysis (IRASA) method is introduced to divide oscillations and fractionations from original EEG data, and parametric methods for the quantitative assessment of brain arousal are further explored [21]. Furthermore, the neuromodulation's effect on arousal levels is revealed through a comparison of the fractal characteristics under pre-stimulation, sham-tDCS and anodal-tDCS.

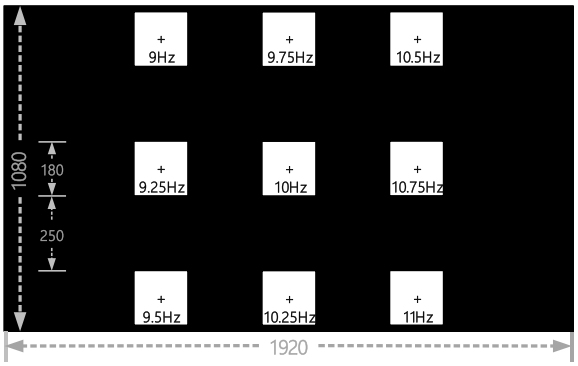

Fig. 1. Parameter settings of SSVEP stimulation.

This study's contributions are summarized below. First, a tDCS-based neuromodulation technique is investigated to modulate brain states and influence EEG properties, contributing to the improvement of SSVEP-BCI performance and the overall utility of BCIs. Second, a brain state estimation method that has never been used in SSVEP-BCI is introduced to assess neuromodulation-induced changes in brain arousal, reducing the drawback of poor robustness of traditional narrow-band energy methods. Third, the use of a parameter-based quantitative representation of brain state is explored, which is an approach that may be used for brain arousal assessment and the modeling of EEGs in SSVEP-BCI.

II. Methods

A. Subjects

Eleven (four of the whole group with ages ranging from 18 to 25 years old, with an average age of 22) and thirteen (4 of the whole group with ages ranging from 20 to 26 years old, with an average age of 23) healthy subjects with corrected-to-normal or normal vision attended the offline and online experiments, respectively. All participants were right-handed. All participants provided informed consent forms before the experiments and were compensated monetarily. The study was approved by the Institutional Review Board of Tsinghua University (application number: 20180041, Jan. 3, 2019).

B. SSVEP Stimulation Settings

A 23.6-inch liquid-crystal display screen (resolution: 1920 × 1080 pixels, refresh rate: 60 Hz) was employed to display SSVEP stimuli (see Fig. 1). Nine 180 × 180-pixel blocks within a black background (RGB: (0, 0, 0)) were used to render the stimuli, with a distance of 250 pixels between adjacent blocks. A black cross in the middle of each stimulus was used to cue the gaze focus position. Subjects had a gaze distance of approximately 80 cm to the screen.

SSVEP stimulations were encoded using the sampled sinusoidal stimulation method [22], [23]. The nine targets were encoded with an initial phase of 0 and frequencies of 9 Hz, 9.75 Hz, 10.5 Hz, 9.25 Hz, 10 Hz, 10.75 Hz, 9.5 Hz, 10.25 Hz and 11 Hz, respectively.

C. tDCS Stimulation

A commercial tDCS stimulator (neuroConn DC Stimulator Plus, Germany) was adopted in this study. The cathodal and anodal tDCS electrodes were respectively placed at the Cz and Oz positions, in accordance with the international 10-20 EEG system) (see Fig. 2) [24], [25]. The dimensions of the tDCS electrodes were 7×5 cm^2. The participants did not need to perform any specific tasks during tDCS stimulation; they were only asked to remain relaxed. The tDCS procedure was tolerated well by all participants, with no adverse effects during or after the experiments.

D. EEG Acquisition

A synamps2 system (Neuroscan, Inc.) was used for the acquisition of EEG data at a sampling rate of 1000 Hz. EEG data were first pre-processed using a band-pass filter from 1 to 100 Hz and then filtered using a notch filter (50 Hz) to eliminate interference at industrial frequencies. The international 10-20 system was employed for the placement of all nine electrodes (O2, Pz, PO5, PO4, Oz, PO3, O1, POz, PO6). The EEG data on the nine electrodes were recoded with impedances lower than 10 kΩ. The reference electrode was placed at the vertex.

E. EEG Analysis

The influence of tDCS-based neuromodulations on EEG characteristics was analyzed. The offline experiment was conducted to compare responses to anodal-tDCS, sham-tDCS and pre-stimulation under different parameters such as SSVEP amplitude, classification accuracy and energy distribution of spontaneous EEG. The online experiment further validated the effect of the optimal tDCS parameters on classification accuracy.

The envelopes of different neuromodulation modes were also compared. Event triggers were used to mark the start time of each trial during the stimulation process and to intercept EEG epochs. Depending on the triggers, EEG data from -0.5s to 4.5s were intercepted to show the entire course of changes under each mode. The Hilbert transform was used to extract the SSVEP envelopes using a band-pass filter from $f-1$ to $f+1$, where f was related to the stimulus frequency.

Classification accuracies were compared under the different neuromodulation modes. A delay of 140 ms was used on the classification algorithms to compensate for the delay in the visual pathway [26], and EEG epochs were intercepted from 0.14 s to $(t+0.14)$ s, where time 0 was the start time of the stimulus, t was the data length (from 0.1 to 4.0 s in the offline experiment and from 0.1 s to 1.5 s in the online experiment with a step of 0.1 s). The training-free method of Filter Bank Canonical Correlation Analysis (FBCCA) [27] and training-required method of Task-Related Component Analysis (TRCA) [28] were adopted for the frequency detection of SSVEPs.

The characteristics of brain states were compared under different neuromodulation modes. Irregular-Resampling Auto-Spectral Analysis (IRASA) [21] was introduced to separate the oscillations and fractionations from the original EEG and to mine characteristics associated with power rhythms.

F. IRASA Method

IRASA was employed to separate oscillatory $x(t)$ and fractal activities $f(t)$ from the original EEG $y(t)$, as shown in equation (1):

$$y(t) = f(t) + x(t) \tag{1}$$

SSVEP and spontaneous EEG were correlated with oscillatory and fractal activity, respectively. The IRASA results reflected the features of the power rhythms associated with brain neural activities.

IRASA exploits the frequency features of the oscillations as well as the self-affine features of the fractals [21]. The original EEG spectrum was first resampled using a range of factors, and then an estimate of the fractal spectrum was obtained through the median of the resampled results. The fractal spectrum was subtracted from the original spectrum to obtain the oscillatory spectrum. A linear function was obtained by fitting the fractal spectrum with the least-squares estimate on the logarithmic scale. The "offset" and "exponent" refer to the log-power intercept and the slope of the fitted linear function, separately. The single-trial EEGs ([0 4] s) of the offline experiments were used as inputs to IRASA to perform feature extraction, and the fractal linear curves were fitted in the frequency range of [1 50] Hz. A statistical and comparative study was conducted under different experimental modes to verify the effectiveness of tDCS-based neuromodulation.

G. Statistical Analysis

SPSS Statistics of IBM Corporation was used for statistical analysis. One-way repeated-measures analysis of variance (ANOVA) was employed to test for differences in EEG classification under the different neuromodulation modes. If the data did not fit the sphericity assumption (assessed using Mauchly's test of sphericity), the Greenhouse–Geisser correction was applied. All pairwise comparisons were Bonferroni-corrected. Statistical significance was defined as $p < 0.05$.

III. Offline Experiment

A. Experimental Setting

Figure 2(a) displays the procedure of the offline experiment. First, a block of SSVEP stimulation tasks was performed as pre-stimulation EEG data were recorded. Second, subjects received sham-tDCS stimulation lasting 21 minutes. The sham-tDCS parameters were such that the stimulation current increased from 0 to 2 mA over 30 s, remained at 2 mA for 30 s, and finally decreased from 2 mA to 0 mA over 30 s. During the

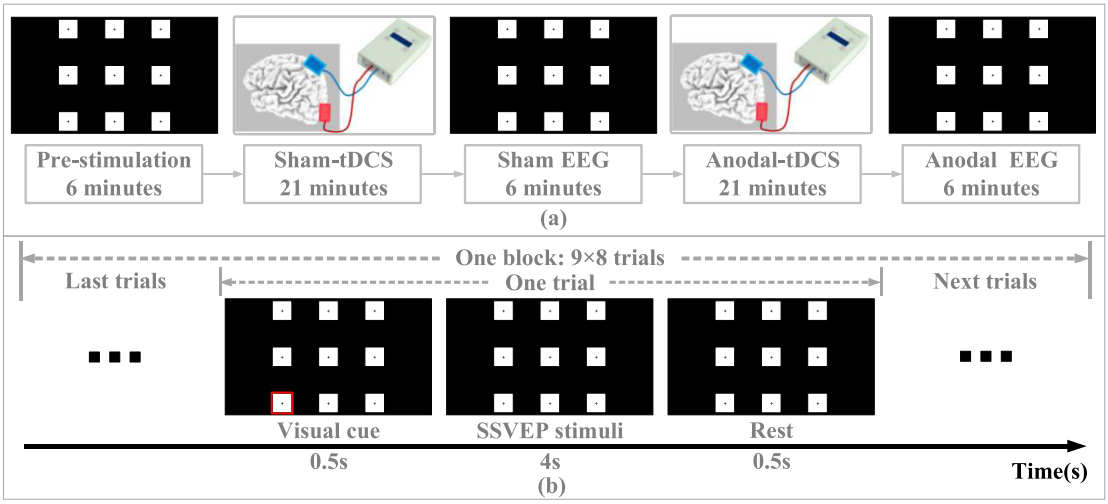

Fig. 2. Parameter settings in the offline experiment. (a) The process of offline experiment. (b) The flowchart of SSVEP in each block.

remaining 19.5 min, tDCS was inactive. Then, another SSVEP stimulation task was performed with the tDCS electrodes removed. The other electrodes' impedances were confirmed to be below 10 kΩ, and sham EEG data were recorded. Fourth, subjects received anodal-tDCS stimulation for 21 minutes, where the stimulation current increased from 0 to 2 mA over 30 s, remained at 2 mA for 20 min, and finally decreased from 2 mA to 0 over 30 s. This design was similar to that of a previous study [29]. Fifth, a third set of SSVEP stimulation was performed with the tDCS electrodes removed. The other electrodes' impedances were verified to be lower than 10 kΩ, and anodal EEG was acquired. The modes of sham-tDCS and anodal-tDCS were the same as those of our previous study [30]. In this paper, sham-tDCS was performed prior to anodal-tDCS, which was a similar sequence to previous tDCS-relevant studies [31], [32].

The procedure of SSVEP stimulation for the offline experiments was as follows (see Fig. 2(b)). Each set comprised 72 trials (9 frequencies × 8 repetitions), which were presented in random sequence. For the first 0.5 s of each trial, a visual cue in the form of a red rectangle was presented around the target stimulus, at which point the participants were to focus their attention. After the cue time, the red rectangle disappeared and all nine targets started flashing for 4 s, during which time the participants were required to focus on the black cross of the target and ignore the other stimuli. There was a 0.5 s interval between trials, during which the screen stopped flashing; the participants could use this interval for a short break. During visual stimulation, a red triangle below the target was used to indicate the location the participants needed to focus on, and subjects were asked to avoid blinking. Each trial lasted 5 s and each set lasted 6 minutes.

B. Results

1) SSVEP Amplitudes: Figure 3 shows the nine channel averaged envelopes of the fundamental-frequency SSVEPs. Pairwise comparisons indicated that the pre-stimulation amplitudes were lower than those of anodal-tDCS ($p < 0.05$, [719:812] ms), and the amplitudes of sham-tDCS were lower than those in anodal-tDCS ($p < 0.05$, [696:1218 1854:2054] ms). Pairwise comparisons at each frequency indicated that the pre-stimulation amplitudes were lower than those of sham-tDCS at 9.25 Hz ($p < 0.05$, [64:283] ms) and 10 Hz ($p < 0.05$, [149:529] ms). The pre-stimulation amplitudes were lower than those of anodal-tDCS at 10.5 Hz ($p < 0.05$, [646:1021] ms), 10 Hz ($p < 0.05$, [0:529] ms) and 10.75 Hz ($p < 0.05$, [775:954] ms). The sham-tDCS amplitudes were lower than those of anodal-tDCS at 10.5 Hz ($p < 0.05$, [704:1132] ms), 10.75 Hz ($p < 0.05$, [107:313] ms), 9.5 Hz ($p < 0.05$, [562:2225] ms), 10.25 Hz ($p < 0.05$, [639:2106] ms) and 11 Hz ($p < 0.05$, [468:759] ms).

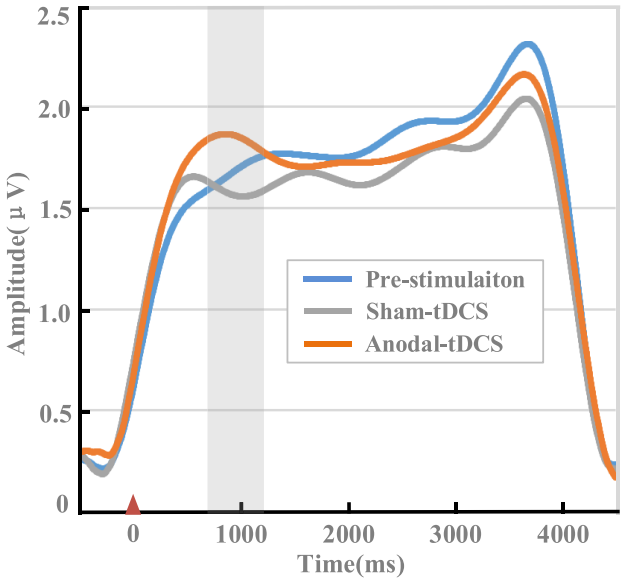

Fig. 3. Averaged envelopes of the nine fundamental-frequency SSVEPs. Time ranges with significant differences are marked with gray shading.

Figure 4 shows the nine-channel averaged amplitudes of the fundamental-frequency SSVEPs after accounting for the visual system delay. In Fig. 4(a), it can be seen that the pre-stimulation amplitudes were lower than those of sham-tDCS at 10 Hz ($p = 0.0208$) and of anodal-tDCS at 10.5 Hz ($p = 0.0144$) and 10 Hz ($p = 0.05$), while the sham-tDCS amplitudes were lower than those of anodal-tDCS at 9 Hz

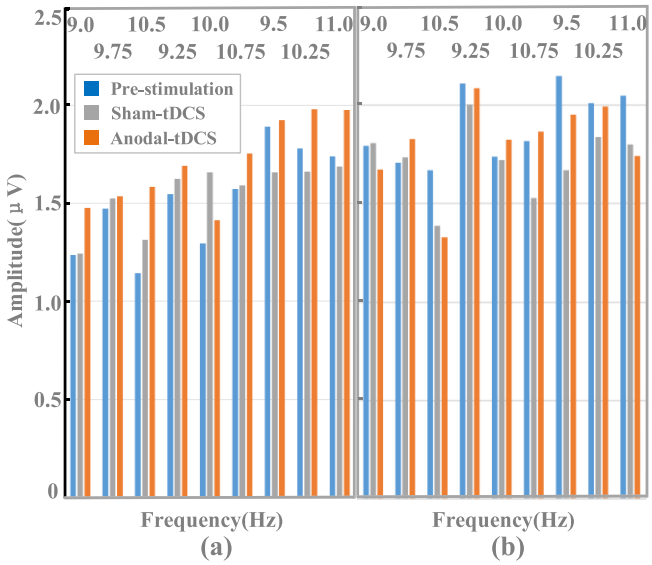

Fig. 4. Averaged amplitudes of the nine fundamental-frequency SSVEPs. (a) [0 1000]ms, (b) [1001 4000]ms.

($p = 0.0467$), 9.5 Hz ($p = 0.0138$), and 10.25 Hz ($p = 0.0347$). In Fig 4(b), the pre-stimulation and anodal-tDCS amplitudes are larger than those of sham-tDCS at 9.25 Hz ($p = 0.02$), 10.0 Hz ($p = 0.0377$), 9.5 Hz ($p = 0.0188$), and 10.75 Hz ($p = 0.0143$), 9.5 Hz ($p = 0.0164$), 10.25 Hz ($p = 0.0056$), respectively.

2) Classification Accuracy: Figure 5 shows the information translate rates (ITRs) (b,d) and accuracies (a,c) of the FBCCA (a,b) and TRCA (c,d) methods. One-way repeated ANOVA among pre-stimulation, sham-tDCS and anodal-tDCS indicates that there were statistically significant differences of the TRCA accuracies for the EEG data lengths of 300 ms ($F(2, 20) = 3.975$, $p = 0.035$) and 500 ms ($F(1.226, 12.256) = 5.31$, $p = 0.014$). Pairwise comparisons of the TRCA results indicated that the pre-stimulation accuracies were lower than those of sham-tDCS at the data lengths of 1600 ms, 1700 ms, 1900 ms, 2000 ms, 2800 ms ($p = 0.0480$, 0.0335, 0.0265, 0.0265, 0.0190, respectively). The accuracies and ITRs of pre-stimulation were lower than those of anodal-tDCS at the data lengths of 400 ms, 500 ms, 700 ms, 800 ms, 900 ms, 1400 ms, 1600 ms, 1800 ms, 1900 ms, 2400 ms ($p = 0.0452$, 0.0193, 0.0220, 0.0356, 0.0414, 0.0265, 0.0260, 0.0480, 0.0265, 0.0266). The accuracies and ITRs of sham-tDCS were lower than those of anodal-tDCS at the data lengths of 300 ms, 400 ms, 500 ms, 700 ms ($p = 0.0217$, 0.0174, 0.0006, 0.0185). Another pairwise comparison of the FBCCA results indicated that the pre-stimulation accuracies and ITRs were lower than those of sham-tDCS at the data length of 1300 ms, 1400 ms, 2100 ms ($p = 0.0359$, 0.0408, 0.0444). The accuracies and ITRs under pre-stimulation were lower than those under anodal-tDCS at the data lengths of 500 ms, 600 ms, [1100:1800] ms, 2000 ms, 2200 ms ($p = 0.0491$, 0.0419, 0.0292, 0.0346, 0.0303, 0.0148, 0.0426, 0.0455, 0.0420, 0.0279, 0.0341, 0.0318). The accuracies and ITRs of sham-tDCS were lower than those of anodal-tDCS at the data lengths of 500 ms, 600 ms, 1500 ms ($p = 0.0048$, 0.0445, 0.0499).

3) IRASA Processing: The results of IRASA processing of the EEG data are shown in Fig. 6. In this study, the offset and exponent parameters are employed to estimate the effect of neuromodulation on brain states and further to explain the effect of tDCS on SSVEP characteristics and SSVEP-BCI performance. The power spectral density (PSD) of the original and fractal EEG are represented via the original and fractal curves, separately. The oscillatory curve was generated through the subtraction of the fractal from original curve. The fractal curve was fitted using the power law curve, and its slope is reflected by the exponent parameter, while the ordinate of the intersection of the power law curve with the vertical axis is represented by the offset parameter.

4) Relationship Between Offset and Exponent: Figures 3, 4, and 5 indicate that SSVEP characteristics (amplitude) and SSVEP-BCI performance (accuracy, ITR) were significantly affected by neuromodulation (pre-stimulation, sham-tDCS and anodal-tDCS). In this section, the averaged EEG data of the nine electrodes over the occipital region are analyzed to extract spontaneous EEG features and determine the relationship between offset and exponent. The results of offset under the different neuromodulation modes are analyzed statistically in Fig. 8.

The scatter plots of offset and exponent are displayed in Fig. 7, and show a nearly positive linear relationship for the offset and exponent parameters regardless of the neuromodulation mode. In addition, the scatter plots associated with the three modes are spatially distributed differently. Specifically, anodal-tDCS is related to the smallest offset and exponent, while pre-stimulation is related to the largest offset and exponent. Therefore, the positive linear relationship between offset and exponent indicates that they had a similar role in reflecting brain state properties, a finding which is supported by previous studies [21], [33]. In this study, the offset was selected randomly to investigate the effectiveness of neuromodulation on brain state interventions, as shown in Fig. 8.

5) Modulation of tDCS on Fractal Characteristics: The offset and exponent showed a positive linear relationship in Fig. 7, which suggests that offset and exponent have similar efficacy in characterizing neuromodulation effects. In the following, offset is randomly chosen as an indicator of brain state to study the effect of neuromodulation. The statistical analyses of offset values for the averaged EEG data of the 9 channels are shown in Fig. 8. The neuromodulation modes had significant effects on offset values. First, the averaged offset values (9 Hz, 9.75 Hz, 10.5 Hz, 9.25 Hz, 10 Hz, 10.75 Hz, 9.5 Hz) under sham-tDCS were lower than those of pre-stimulation. For example, the offset values under sham-tDCS (0.2827 ± 0.0467) were significantly lower than those under pre-stimulation (0.3609 ± 0.0484), with $p = 0.0382$. Second, the averaged offset values of the nine frequencies under pre-stimulation were larger than those under anodal-tDCS. For example, the offset values under anodal-tDCS were significantly lower than those under pre-stimulation at 9 Hz ($p = 0.0011$), 9.75 Hz ($p = 0.0047$), 10.5 Hz ($p = 0.0013$), 9.25 Hz ($p = 0.0139$), and 9.5 Hz ($p = 0.0111$). Third, the averaged offset values (all nine frequencies) under sham-tDCS

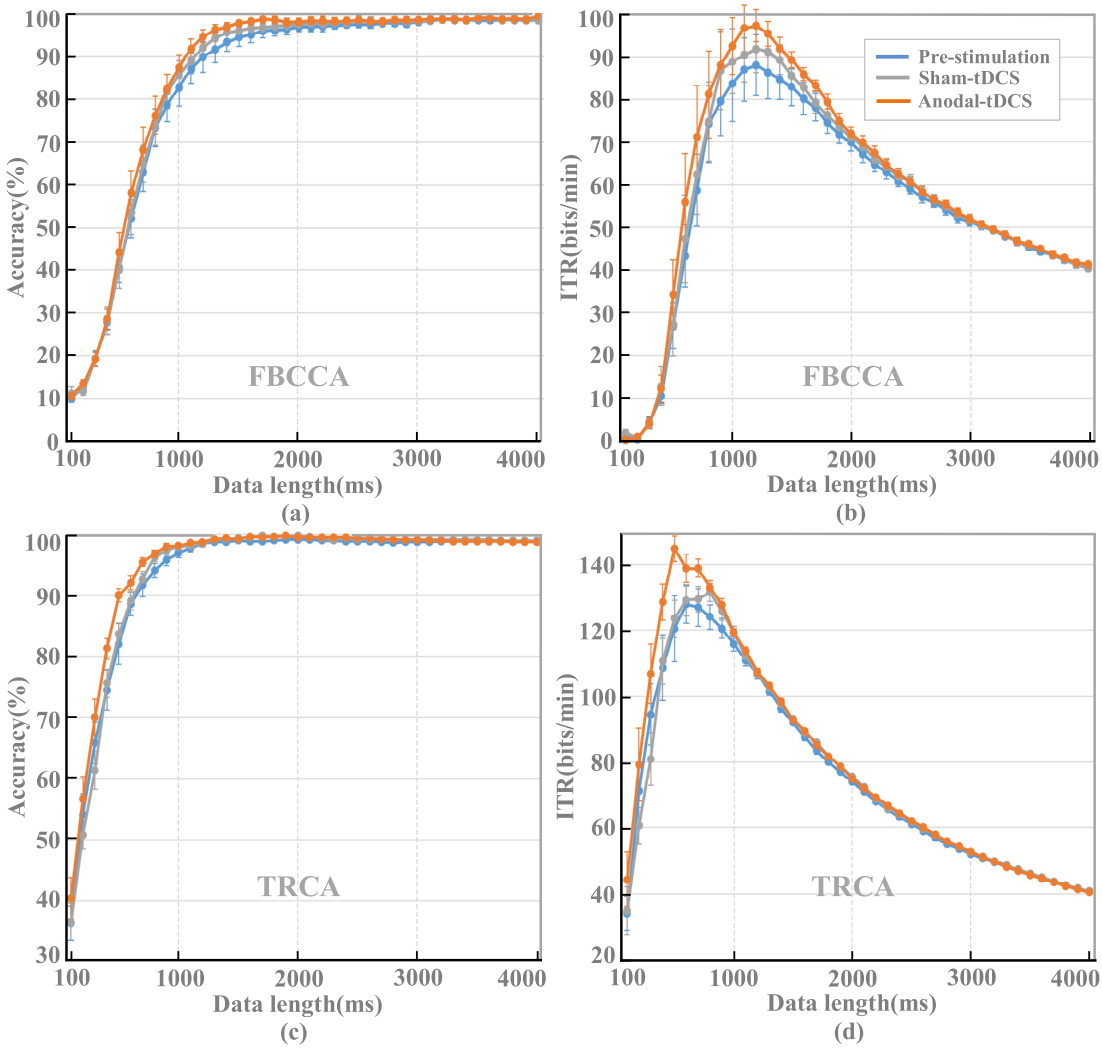

Fig. 5. Offline experiment results. (a)(b) FBCCA method. (c)(d) TRCA method. (a)(c) Classification accuracies. (b)(d) ITRs.

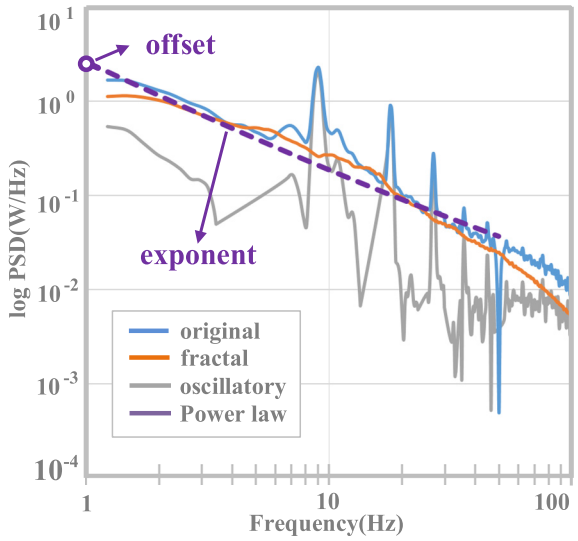

Fig. 6. Processing effect of IRASA on EEG data, which shows the PSD in logarithmic coordinates.

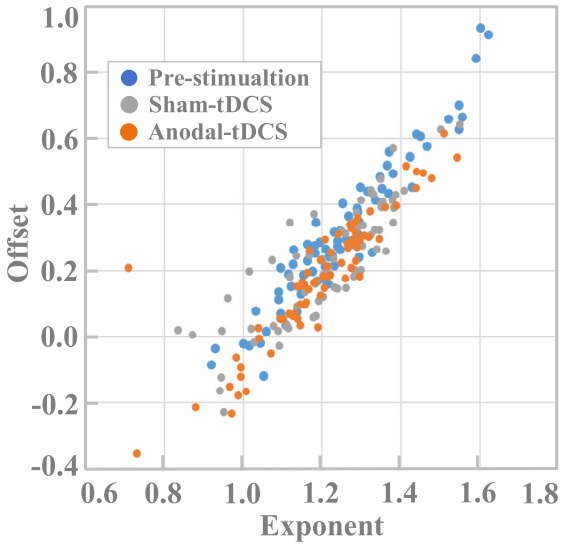

Fig. 7. Offsets and exponents in different neuromodulation modes.

were larger than those under anodal-tDCS. For example, the offset values under sham-tDCS at 9.5 Hz (0.3109 ± 0.0562) were significantly higher than those under anodal-tDCS (0.2409 ± 0.0465), with a significance value of $p = 0.02084$. The above results show that the fractal parameters (offset and exponent) were modulated by tDCS-based neuromodulations,

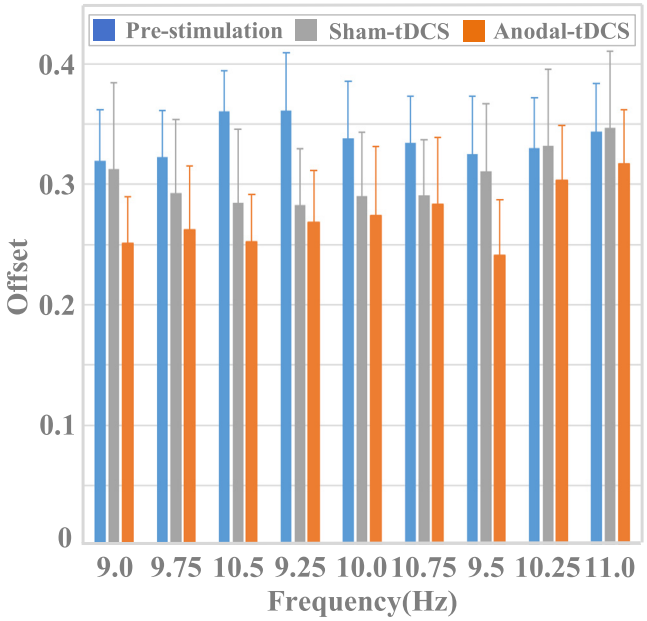

Fig. 8. Statistical results of offset and exponent (error bars referred to the standard errors of the mean).

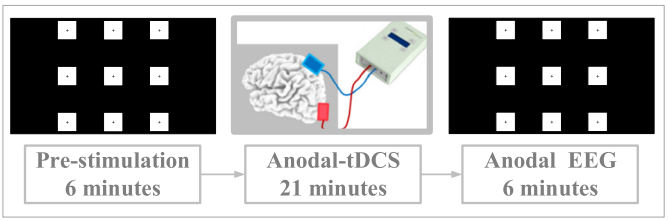

Fig. 9. Online experiment process.

and anodal-tDCS and pre-stimulation on the whole were related to the smallest and largest values, respectively. Similar conclusions as for the offset values were obtained when analyzing the exponent values.

IV. Online Experiment

A. Experimental Setting

Since in the offline experiments induced better SSVEP performance enhancement under anodal-tDCS than under sham-tDCS, during the online experiments sham-tDCS was ignored and the focus was on the further validation of the effectiveness of anodal-tDCS on the performance of SSVEP-BCIs.

The experimental procedure was as follows (Fig. 9). First, two blocks of SSVEP stimulation tasks were performed, with a 1-minute break in-between. Second, participants received anodal-tDCS for a duration of 21 minutes. The parameters of the anodal-tDCS stimulation were the same as those of the offline experiment, i.e. the stimulation current was increased from 0 to 2 mA over 30 s, then remained constant at 2 mA for 20 minutes, and finally decreased from 2 mA to 0 over 30 s. Third, two sets of SSVEP stimulation tasks were performed again, with a 1-minute rest between the two sets.

The experimental equipment and environment used in the online experiments were the same as those of the offline experiments, with the trials (9 frequencies $\times$ 8 repetitions) within each block presented in a random sequence. During the offline experiments, the length of EEG data related to the largest ITR found using FBCCA was around 1.5 s, so the visual stimulation time during the online experiments was set to 1.5 s. The duration of each trial was 2 s (0.5 s for the visual cue of the red rectangle and 1.5 s for the SSVEP stimulus). Different to the offline experiment, during the online experiment a feedback loop was introduced, resulting in a complete closed-loop system. If the target was correctly identified, an audible feedback of "Di" appeared at the end of the trial as a feedback message, while no audible feedback was presented if it was not correctly identified.

B. Results

Figure 10 shows the ITRs (b,d) and classification accuracies (a,c) obtained using FBCCA (a,b) and TRCA (c,d) during the online experiment. Statically significant differences were observed under pre-stimulation and anodal-tDCS. Pairwise comparisons indicated that the averaged accuracies and ITRs under pre-stimulation were significantly lower than those under anodal-tDCS at the data lengths of 700 ms for FBCCA ($p = 0.0384$) and [100 300:800 1000] ms for TRCA ($p = 0.0210$, 0.0471, 0.0018, 0.0090, 0.0273, 0.0054, 0.0081, 0.0299), respectively.

Furthermore, the results of single block were also compared. First, the accuracies and ITRs during the second block of anodal-tDCS were not only significantly larger ($p < 0.05$) than those of the first block of pre-stimulation for TRCA ([300:1000] ms) and FBCCA ([900:1000 1200 1400] ms), but also were significantly larger ($p < 0.05$) than those of the second block of pre-stimulation for TRCA ([600:1000 1200:1400] ms) and FBCCA ([900:1000 1200 1400] ms). Second, the accuracies and ITRs of the second block of anodal-tDCS were significantly larger ($p < 0.05$) than those of the first block of anodal-tDCS for FBCCA ([800:1200] ms) and TRCA ([100 500:1100] ms). Third, the accuracies and ITRs of the first block of anodal-tDCS were significantly larger ($p < 0.05$) than those of the first block of pre-stimulation for TRCA ([100] ms) and FBCCA ([700] ms), and significantly larger than those of the second block of pre-stimulation for TRCA ([100] ms) and FBCCA ([400] ms).

V. Discussion

A. Effect of Neuromodulation on the Characteristics of EEG Oscillatory Components

The effect of neuromodulation on the oscillatory features was analyzed. The focus of the analysis was on the modulation effect of tDCS on the transient-state response of SSVEP, which is closely related to the BCI performance. In fact, in SSVEP-BCIs, the time course of SSVEP can be divided into two periods: transient-state response (TSR) and steady-state response (SSR) [34]. As the periodic stimulation was activated, a TSR appeared and then stabilized to form an SSR waveform that oscillated repeatedly at frequencies associated with the visual stimuli [35], [36], [37], [38]. As signal processing technologies have been improved, the data length used for target identification has been reduced, which has made TSR

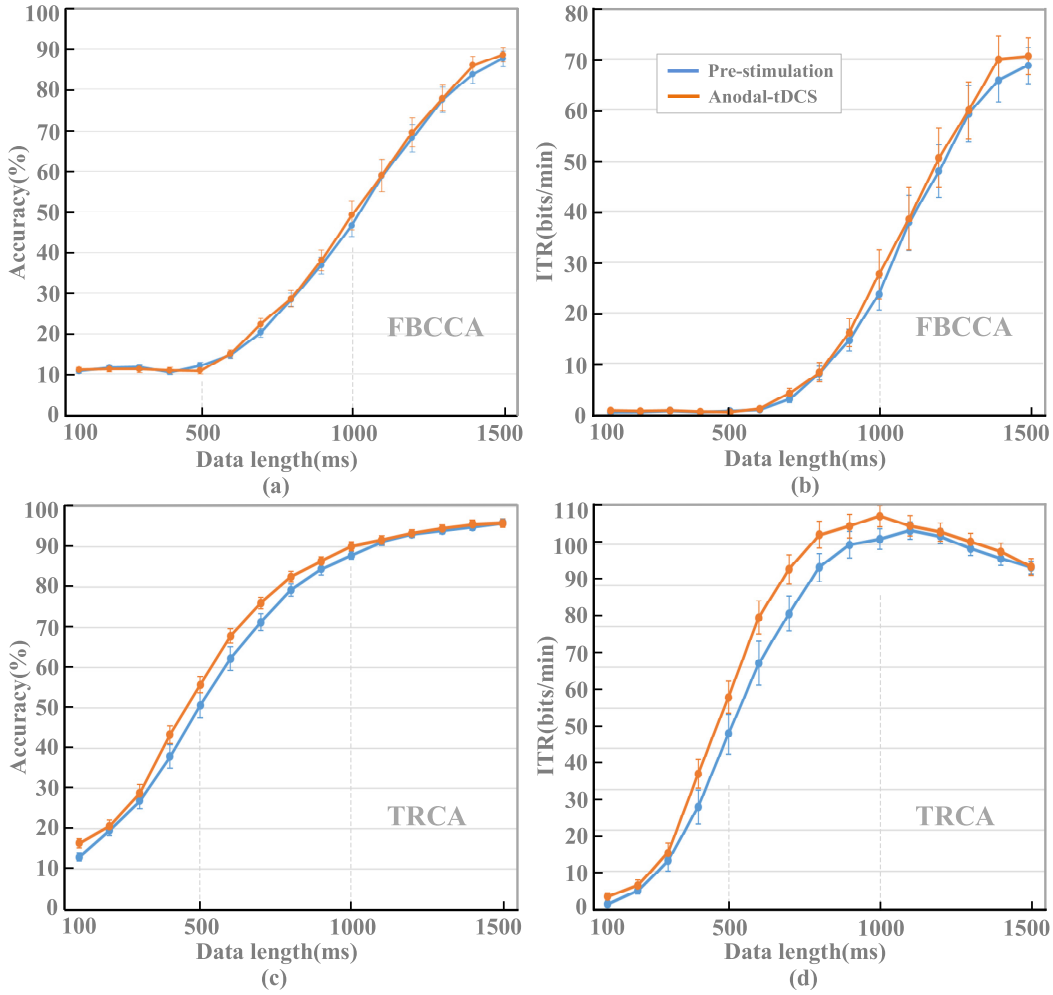

Fig. 10. Online experiment results. (a)(b) FBCCA method. (c)(d) TRCA method. (a)(c) Classification accuracies. (b)(d) ITR.

increasingly important. In this study, the focus is on SSVEPs occurring within [0 1.5] s.

The results indicate that tDCS, and anodal-tDCS in particular, can be used to increase the TSR amplitudes and further enhance SSVEP-BCI performance. Figure 3 shows the effect of tDCS-based neuromodulation on SSVEP envelopes, with anodal-tDCS inducing the strongest TSR. In addition, Fig. 4 demonstrates the advantage of anodal-tDCS in terms of the average SSVEP amplitude within the duration of TSR. Furthermore, Fig. 5 shows the effectiveness of neuromodulation on the enhancement of SSVEP-BCI performance. Finally, Fig. 10 further validates the effectiveness of anodal-tDCS during online experiments, demonstrating its potential to improve BCI performance through brain state intervention. The effectiveness of sham-tDCS is demonstrated, although it is slightly inferior compared to anodal-tDCS.

Anodal-tDCS not only increased the arousal levels of brain states (Fig. 8), but also caused an enhancement of the BCI performance (Figs. 5, 10). The results reflect the positive relationship between brain state arousal and BCI performance, which is also supported by previous studies. For example, the decline of sustained attention and fatigue in BCI usually manifests through slow responses, decreased EEG quality, and reduced classification accuracy [37], [38], [39].

The quality of the EEG data from the offline experiment (Fig. 5) was superior to that of the online experiment (Fig. 10). It is hypothesized that this was mainly due to the completely different participants of the offline and online experiments.

The results that anodal-tDCS enhanced SSVEP responses can be explained via the tDCS mechanism, a technique that regulates neuronal activity in the cerebral cortex [8], [9]. Neurophysiological experiments have demonstrated that neuron response to static electric fields (direct current) was achieved through changes in firing frequency [16], [25]. The spontaneous firing of neurons increases and decreases when anodal-tDCS and cathodal-tDCS are applied to neuronal cells, respectively [29], [30]. Thus, anodic and cathodic stimulations of neurons lead to enhanced and reduced neuronal excitability, respectively, which is ultimately reflected in enhanced and diminished evoked neural responses.

B. Effect of tDCS on Brain States

In this paper, a comparison of the effects of the three experimental modes of pre-stimulation, sham-tDCS and anodal-tDCS, on EEG fractal features is conducted, thus providing evidence to reveal the effect of neuromodulation on brain states.

The results of Fig. 8 demonstrate the sensitivity of fractal features to tDCS-based neuromodulations. On the one hand, anodal-tDCS induced the lowest offset and exponent values. For example, at all nine frequencies, the mean offset under anodal-tDCS was lower than those under pre-stimulation. On the other hand, sham-tDCS also induced a negative effect on the fractal parameters, although it was less significant than that of anodal-tDCS. The results suggest that the fractal component properties can be modulated via tDCS-based neuromodulation, as both sham-tDCS and anodal-tDCS showed negative modulation of the offset and exponent values, especially the latter.

The results reflect the modulatory effect of tDCS neuromodulation on brain states. The fractal parameters are quantitative descriptions of the EEG power law characteristics, where the exponential or offset values are roughly positively correlated with the share of low-frequency energy in the power law, i.e. larger exponent or offset values correspond to more low-frequency energy components in the power law, and vice versa. On the other hand, the energy distribution of the power law has been shown to be a valid measure of brain state [4], [40]. For example, the exponent of $1/f$ activity shows a roughly positive relationship with sleep depth [41], [42]. The main components of the EEG were theta, delta and alpha oscillations in the N1, N3 sleep and awake states, separately. EEG features associated with fatigue states include increases in delta and theta activities and reduced power in beta activity [43]. Overall, the increase in the level of brain state arousal tends to be accompanied by a reduction of low-frequency energy and a growth in high-frequency energy. Therefore, the power law features can be explored as indicators to measure brain states at different arousal levels.

In this study, tDCS-based neuromodulation induced smaller offset and exponent values, which reflects increased arousal levels of brain states. Since the fractional or offset values were negatively and positively correlated with high-frequency and low-frequency energies, respectively, tDCS-based neuromodulation induced a reduction in low-frequency energy and a growth in high-frequency energy, signaling an increase in the brain state arousal level. This conclusion is supported by previous studies. For example, fractal parameters have been used to describe changes in brain states during the process of rapid serial visual presentation (RSVP)-BCI, with offset and exponent values increasing with increasing fatigue and decreasing sustained attention [33]. Transcranial electrical stimulation causes a decrease in reaction times and a simultaneous increase in skin conductance, which suggests a general increase in brain state arousal [44].

C. Effectiveness of IRASA Method

SSVEP-BCI researchers tend to focus on oscillatory properties and ignore the fractal properties. In fact, fractal EEG properties are potential indicators useful for brain state assessment in BCIs. The separation of oscillations and fractal components is an important problem for scholars in the field of SSVEP-BCIs.

In this paper, IRASA is employed to extract the fractal oscillations and fractals from original EEG. Specifically, Fig. 6 demonstrates the effect of IRASA on the extraction of the spectral features of the fractal components. As a result, the fractal components are fitted to curves that are characterized by parameters (offset and exponent). The curve-fitting is robust and intuitive compared to conventional methods because it reflects the variation of EEG energy with the frequency of interest ([1 50] Hz). In addition, parameters (offset and exponent) are used to characterize the spectral characteristics of the fractal components in quantitative, which better promotes and facilitates the assessment and comparison of various brain states induced by neuromodulation. Figure 7 indicates the relationship between offline and exponent, and Fig. 8 further verifies that the offset is effective in characterizing the different brain states induced by neuromodulation. The findings suggest that parameters such as offset or exponent can reflect variations in fractal EEG quantitatively and are valid indicators for assessing neuromodulation-induced brain states, indicating the validity of IRASA.

D. Expected Applications

The expected applications of the proposed method are demonstrated through the following points. First, it is expected that the method will be used for the improvement of BCI performance. This study validates the effectiveness of neuromodulation, specifically anodal-tDCS, in enhancing the arousal level of brain states and improving SSVEP-BCI performance, and therefore provides insight into BCI performance improvement based on state intervention and enhances the practicality of BCI systems.

Second, the method is expected to be used in the brain state evaluation using BCIs. The oscillations and fractals are extracted through IRASA and their properties are compared under the pre-stimulation, sham-tDCS and anodal-tDCS. The results reflect the effect of brain state on fractal EEGs. This study demonstrates that the parameters (offset and exponent) of the fractal components can be used as valid brain state evaluation indicators.

Third, it is expected that the method will be used for EEG modeling. In previous EEG modeling studies in the field of BCIs, the fractal component was neglected, which has led to inaccurate EEG models. In addition, the effect of brain state on EEG models was neglected. By involving the characteristics of fractals as well as the influence of brain state, EEG modeling is expected to be improved.

E. Possible Improvements

This study can be expanded in the following ways. First, the stimulation frequencies can be expanded to verify the effect of tDCS under different frequencies. Second, more subjects can be involved to ensure the robustness of the tDCS results. Third, this study did not investigate the duration of the improvement effect on SSVEP-BCI after tDCS stimulation, and this will be the focus of ensuing studies.

VI. Conclusion

In this study, a neuromodulation technology based on transcranial direct current stimulation is explored with the aim of enhancing the performance of SSVEP-BCIs. The findings

provide insight into the enhancement of BCI performance based on personal state interventions, as well as an effective method for quantitative brain state monitoring.

REFERENCES

[1] X. Gao, Y. Wang, X. Chen, and S. Gao, "Interface, interaction, and intelligence in generalized brain–computer interfaces," *Trends Cognit. Sci.*, vol. 25, no. 8, pp. 671–684, Aug. 2021.

[2] Z. Wang, C. M. Wong, A. Rosa, T. Qian, T.-P. Jung, and F. Wan, "Stimulus-stimulus transfer based on time-frequency-joint representation in SSVEP-based BCIs," *IEEE Trans. Biomed. Eng.*, vol. 70, no. 2, pp. 603–615, Feb. 2023.

[3] S. Zhang, Y. Chen, L. Zhang, X. Gao, and X. Chen, "Study on robot grasping system of SSVEP-BCI based on augmented reality stimulus," *Tsinghua Sci. Technol.*, vol. 28, no. 2, pp. 322–329, Apr. 2023.

[4] U. Talukdar, S. M. Hazarika, and J. Q. Gan, "Adaptive feature extraction in EEG-based motor imagery BCI: Tracking mental fatigue," *J. Neural Eng.*, vol. 17, no. 1, Jan. 2020, Art. no. 016020.

[5] X. Zheng et al., "Anti-fatigue performance in SSVEP-based visual acuity assessment: A comparison of six stimulus paradigms," *Frontiers Human Neurosci.*, vol. 14, p. 301, Jul. 2020.

[6] E. Chew et al., "Using transcranial direct current stimulation to augment the effect of motor imagery-assisted brain-computer interface training in chronic stroke patients—Cortical reorganization considerations," *Frontiers Neurol.*, vol. 11, p. 948, Aug. 2020.

[7] M. Ortiz, E. Iáñez, J. A. Gaxiola-Tirado, D. Gutiérrez, and J. M. Azorín, "Study of the functional brain connectivity and lower-limb motor imagery performance after transcranial direct current stimulation," *Int. J. Neural Syst.*, vol. 30, no. 8, Aug. 2020, Art. no. 2050038.

[8] N. Kaongoen, J. Jeon, and S. Jo, "Enhancing the performance of P300-based BCIs by tDCS of the left VL-PFC," in *Proc. 10th Int. Winter Conf. Brain-Comput. Interface (BCI)*, Feb. 2022, pp. 1–5.

[9] A. Izzidien, S. Ramaraju, M. A. Roula, and P. W. McCarthy, "Effect of anodal-tDCS on event-related potentials: A controlled study," *BioMed Res. Int.*, vol. 2016, Nov. 2016, Art. no. 1584947.

[10] B. S. Baxter, B. J. Edelman, A. Sohrabpour, and B. He, "Anodal transcranial direct current stimulation increases bilateral directed brain connectivity during motor-imagery based brain–computer interface control," *Frontiers Neurosci.*, vol. 11, p. 691, Dec. 2017.

[11] D.-W. Kim, E. Kim, C. Lee, and C.-H. Im, "Can anodal transcranial direct current stimulation increase steady-state visual evoked potential responses?" *J. Korean Med. Sci.*, vol. 34, no. 43, p. e285, 2019.

[12] B. Liu et al., "Effects of transcranial direct current stimulation on steady-state visual evoked potentials," in *Proc. 39th Annu. Int. Conf. IEEE Eng. Med. Biol. Soc. (EMBC)*, Jul. 2017, pp. 2126–2129.

[13] M. A. Nitsche et al., "Modulation of cortical excitability by weak direct current stimulation—Technical, safety and functional aspects," *Supplements Clin. Neurophysiology*, vol. 56, pp. 255–276, Jan. 2003.

[14] W. Paulus, "Outlasting excitability shifts induced by direct current stimulation of the human brain," *Suppl. Clin. Neurophysiol.*, vol. 57, pp. 708–714, Jan. 2004.

[15] N. Accornero, P. Li Voti, M. La Riccia, and B. Gregori, "Visual evoked potentials modulation during direct current cortical polarization," *Exp. Brain Res.*, vol. 178, no. 2, pp. 261–266, Mar. 2007.

[16] A. L. Mangia, M. Pirini, and A. Cappello, "Transcranial direct current stimulation and power spectral parameters: A tDCS/EEG co-registration study," *Frontiers Human Neurosci.*, vol. 8, p. 601, Aug. 2014.

[17] S. K. L. Lal and A. Craig, "A critical review of the psychophysiology of driver fatigue," *Biol. Psychol.*, vol. 55, no. 3, pp. 173–194, Feb. 2001.

[18] E. Wascher et al., "Frontal theta activity reflects distinct aspects of mental fatigue," *Biol. Psychol.*, vol. 96, pp. 57–65, Feb. 2014.

[19] S. Kar, M. Bhagat, and A. Routray, "EEG signal analysis for the assessment and quantification of driver's fatigue," *Transp. Res. F, Traffic Psychol. Behaviour*, vol. 13, no. 5, pp. 297–306, Sep. 2010.

[20] J. Min, P. Wang, and J. Hu, "Driver fatigue detection through multiple entropy fusion analysis in an EEG-based system," *PLoS ONE*, vol. 12, no. 12, Dec. 2017, Art. no. e0188756.

[21] H. Wen and Z. Liu, "Separating fractal and oscillatory components in the power spectrum of neurophysiological signal," *Brain Topography*, vol. 29, no. 1, pp. 13–26, Jan. 2016.

[22] S. Zhang, X. Gao, and X. Chen, "Humanoid robot walking in maze controlled by SSVEP-BCI based on augmented reality stimulus," *Frontiers Hum. Neurosci.*, vol. 16, Jul. 2022, Art. no. 908050.

[23] G. Ming, W. Pei, H. Chen, X. Gao, and Y. Wang, "Optimizing spatial properties of a new checkerboard-like visual stimulus for user-friendly SSVEP-based BCIs," *J. Neural Eng.*, vol. 18, no. 5, Oct. 2021, Art. no. 056046.

[24] A. Antal, T. Z. Kincses, M. A. Nitsche, O. Bartfai, and W. Paulus, "Excitability changes induced in the human primary visual cortex by transcranial direct current stimulation: Direct electrophysiological evidence," *Investigative Ophthalmology Vis. Sci.*, vol. 45, pp. 702–707, Feb. 2004.

[25] T. Neuling, S. Wagner, C. H. Wolters, T. Zaehle, and C. S. Herrmann, "Finite-element model predicts current density distribution for clinical applications of tDCS and tACS," *Frontiers Psychiatry*, vol. 3, p. 83, Sep. 2012.

[26] X. Chen, Y. Wang, M. Nakanishi, X. Gao, T.-P. Jung, and S. Gao, "High-speed spelling with a noninvasive brain–computer interface," *Proc. Nat. Acad. Sci. USA*, vol. 112, no. 44, pp. 6058–6067, Nov. 2015.

[27] X. Chen, Y. Wang, S. Gao, T.-P. Jung, and X. Gao, "Filter bank canonical correlation analysis for implementing a high-speed SSVEP-based brain–computer interface," *J. Neural Eng.*, vol. 12, no. 4, Aug. 2015, Art. no. 046008.

[28] M. Nakanishi, Y. Wang, X. Chen, Y. Wang, X. Gao, and T.-P. Jung, "Enhancing detection of SSVEPs for a high-speed brain speller using task-related component analysis," *IEEE Trans. Biomed. Eng.*, vol. 65, no. 1, pp. 104–112, Jan. 2018.

[29] M. A. K. Peters, B. Thompson, L. B. Merabet, A. D. Wu, and L. Shams, "Anodal tDCS to v1 blocks visual perceptual learning consolidation," *Neuropsychologia*, vol. 51, no. 7, pp. 1234–1239, Jun. 2013.

[30] G. Dong, Y. Wang, and X. Chen, "Anodal occipital tDCS enhances spontaneous alpha activity," *Neurosci. Lett.*, vol. 721, Mar. 2020, Art. no. 134796.

[31] C. Peña-Gómez et al., "Modulation of large-scale brain networks by transcranial direct current stimulation evidenced by resting-state functional MRI," *Brain Stimulation*, vol. 5, no. 3, pp. 252–263, Jul. 2012.

[32] G. F. Spitoni, R. L. Cimmino, C. Bozzacchi, L. Pizzamiglio, and F. D. Russo, "Modulation of spontaneous alpha brain rhythms using low-intensity transcranial direct-current stimulation," *Frontiers Hum. Neurosci.*, vol. 7, p. 529, Sep. 2013.

[33] S. Zhang, X. Yan, Y. Wang, B. Liu, and X. Gao, "Modulation of brain states on fractal and oscillatory power of EEG in brain–computer interfaces," *J. Neural Eng.*, vol. 18, no. 5, Oct. 2021, Art. no. 056047.

[34] S. Zhang, X. Han, X. Chen, Y. Wang, S. Gao, and X. Gao, "A study on dynamic model of steady-state visual evoked potentials," *J. Neural Eng.*, vol. 15, no. 4, Aug. 2018, Art. no. 046010.

[35] D. Regan, "Some characteristics of average steady-state and transient responses evoked by modulated light," *Electroencephalogr. Clin. Neurophysiol.*, vol. 20, no. 3, pp. 238–248, Mar. 1966.

[36] D. Regan, "Recent advances in electrical recording from the human brain," *Nature*, vol. 253, no. 5491, pp. 401–407, Feb. 1975.

[37] S. Zhang, J. Sun, and X. Gao, "The effect of fatigue on brain connectivity networks," *Brain Sci. Adv.*, vol. 6, no. 2, pp. 120–131, Jun. 2020.

[38] S. Zhang and X. Chen, "Effect of background luminance of visual stimulus on elicited steady-state visual evoked potentials," *Brain Sci. Adv.*, vol. 8, no. 1, pp. 50–56, Mar. 2022.

[39] S. Ajami, A. Mahnam, and V. Abootalebi, "An adaptive SSVEP-based brain-computer interface to compensate fatigue-induced decline of performance in practical application," *IEEE Trans. Neural Syst. Rehabil. Eng.*, vol. 26, no. 11, pp. 2200–2209, Nov. 2018.

[40] Y. Peng, C. M. Wong, Z. Wang, A. C. Rosa, H. T. Wang, and F. Wan, "Fatigue detection in SSVEP-BCIs based on wavelet entropy of EEG," *IEEE Access*, vol. 9, pp. 114905–114913, 2021.

[41] E. Pereda, A. Gamundi, R. Rial, and J. González, "Non-linear behaviour of human EEG: Fractal exponent versus correlation dimension in awake and sleep stages," *Neurosci. Lett.*, vol. 250, no. 2, pp. 91–94, Jun. 1998.

[42] V. Miskovic, K. J. MacDonald, L. J. Rhodes, and K. A. Cote, "Changes in EEG multiscale entropy and power-law frequency scaling during the human sleep cycle," *Human Brain Mapping*, vol. 40, no. 2, pp. 538–551, Feb. 2019.

[43] Y. Tran, A. Craig, R. Craig, R. Chai, and H. Nguyen, "The influence of mental fatigue on brain activity: Evidence from a systematic review with meta-analyses," *Psychophysiology*, vol. 57, no. 5, May 2020, Art. no. e13554.

[44] P. Mauri, C. Miniussi, M. Balconi, and D. Brignani, "Bursts of transcranial electrical stimulation increase arousal in a continuous performance test," *Neuropsychologia*, vol. 74, pp. 127–136, Jul. 2015.